The telomerase inhibitor AZT enhances differentiation and prevents overgrowth of human pluripotent stem cell–derived neural progenitors

Received for publication, August 4, 2017, and in revised form, March 27, 2018 Published, Papers in Press, April 8, 2018, DOI 10.1074/jbc.M117.809889

Yao Hu[‡§¶], Kai-Heng Fang[§], Lu-Ping Shen[§], Shi-Ying Cao[§], Fang Yuan[§], Yuwen Su[§], Min Xu[§], Yufeng Pan[‖], Yaoyu Chen[1], and Yan Liu[‡§¶2]**

*From the [‡]State Key Laboratory of Reproductive Medicine, [§]Institute for Stem Cell and Neural Regeneration, School of Pharmacy, and [¶]Collaborative Innovation Center for Cardiovascular Disease Translational Medicine, Nanjing Medical University, Nanjing 211166, China, [‖]The Key Laboratory of Developmental Genes and Human Disease, Institute of Life Sciences, Southeast University, Nanjing, Jiangsu 210096, China, and **Division of Hematology, Jiangsu Provincial Traditional Chinese Medical Hospital, Nanjing, Jiangsu Province 210029, China*

Edited by Paul E. Fraser

Human pluripotent stem cell (hPSC)–based cell-replacement therapy has emerged as a promising approach for addressing numerous neurological diseases. However, hPSC transplantation has the potential to cause human cell overgrowth and cancer, which represents a major obstacle to implementing hPSC-based therapies. Inhibition of the overgrowth of transplanted cells could help reduce the risk for hPSC transplantation–induced tumorigenesis. In this study, we report that the telomerase inhibitor azidothymidine (3′-azido-3′-deoxythymidine; AZT) enhances the differentiation of cortical neurons and significantly suppresses the proliferation of hPSC-derived cortical progenitors. Using human embryonic stem cells and induced pluripotent stem cells in culture, we found that AZT effectively reduces the number of dividing progenitors without inducing cell death. Furthermore, AZT promoted differentiation of cortical progenitors and maturation of cortical neurons. Of note, AZT-pretreated, hPSC-derived neural progenitors exhibited decreased proliferation and increased differentiation into cortical neurons when transplanted into the mouse brain. In summary, our findings indicate that AZT prevents the overgrowth of hPSC-derived neural precursors and enhances the differentiation of cortical neurons in both cell cultures and hPSC-transplanted mouse brain. We propose that our work could inform clinical applications of hPSC-based cell therapy.

Cell-replacement therapy is a promising therapeutic approach for human neurological disease (1). Human pluripotent stem cells (hPSCs)[3] and induced pluripotent stem cells (iPSCs) may provide an unlimited resource for cell-replacement therapy. hPSCs have the potential to differentiate into neural stem/progenitor cells (NS/PCs) and subsequently be induced to differentiate into three neural lineages, including neurons, astrocytes, and oligodendrocytes (2–6). So far, progress has been made in the development of NS/PCs as a promising cell source for regenerative medicine targeting CNS disorders (4, 7–11). However, a major hurdle for applying this cell source to human disease is that transplantation of certain hPSC-NS/PCs may lead to tumor-like overgrowth and deterioration of neural function during long-term observations (12). For example, hPSC-NS/PCs presented tumor-like overgrowth *in vivo* after transplantation (13, 14). These overgrowth cells contained a great amount of undifferentiated human-specific $NESTIN^+$ cells and enlarged the host brain.

To safely use iPSC-based transplantation therapy in clinical applications, many efforts have been made to prevent tumor-like overgrowth. Removing remnant immature NS/PCs or differentiate these cells into more mature cell types may help to avoid tumor-like overgrowth following transplantation. For instance, a physiological medium (BrainPhys basal + serum-free supplements) with adjustments to the concentrations of inorganic salts, neuroactive amino acids, and energetic substrates improved maturation and enhanced the proportion of synaptically active neurons (15), which reduced tumor-like overgrowth. Another efficient method is to find the key signaling pathway controlling the induction and differentiation of NS/PCs. Inhibition of Notch signaling with a γ-secretase inhibitor (GSI) was shown to be able to induce NS/PCs to develop into a more mature state with limited proliferation *in vitro* (14, 16). In addition, treatment of iPSC-derived dopaminergic progenitor cells with GSIs prior to transplantation may control the growth of a potentially proliferative cell population *in vivo* (16). However, the GSIs caused detrimen-

This work was supported by National Natural Science Foundation of China Grants 81471301, 81301162, 81570141, and 81522001; National Key Research and Development Program of China Grant 2016YFC1306703; Jiangsu Outstanding Young Investigator Program Grant BK20160044; Jiangsu Province Natural Science Foundation Grant BK20130891; and the Jiangsu Province's Innovation program. The authors declare that they have no conflicts of interest with the contents of this article.

This article contains Figs. S1–S6.

[1] To whom correspondence may be addressed. E-mail: yaoyu.chen@njmu.edu.cn.

[2] To whom correspondence may be addressed. E-mail: yanliu@njmu.edu.cn.

[3] The abbreviations used are: hPSC, human pluripotent stem cell; hESC, human ES cell; AZT, azidothymidine; iPSC, induced pluripotent stem cell; hiPSC, human induced pluripotent stem cell; NS/PCs, neural stem/progenitor cells; GSI, γ-secretase inhibitor; TERT, telomerase reverse transcriptase; EdU, 5-ethynyl-2′-deoxyuridine; iPS, induced pluripotent stem; DAPT, *N*-[*N*-(3,5-difluorophenacetyl)-L-alanyl]-*S*-phenylglycine *t*-butyl ester; CCK-8, Cell Counting Kit-8; HN, human nuclei; NIM, neural induction medium.

tal effects in patients with Alzheimer's disease, and the toxic side effects are the main concern for clinical application of this tool compound (17).

It is important to find a way to optimize the induction and differentiation of NS/PCs. Azidothymidine (3′-azido-3′-deoxythymidine; AZT), a telomerase inhibitor, could inhibit the telomerase reverse transcriptase (TERT) and interrupted the cell proliferation (18). Our previous study showed that AZT disrupted the proliferation of adult neural stem cells in the subventricular zone and hippocampus in mice without causing cell damage or apoptosis (19, 20). However, the effects of AZT in hPSC-derived neurons have not yet been explored. In this study, we show that the telomerase inhibitor AZT suppressed the proliferation of hPSC-derived neural progenitors, promoted the differentiation of hPSC-derived cortical neurons, and enhanced the maturation of hPSC-derived neurons. Furthermore, we also found that AZT-pretreated, hPSC-derived precursors inhibited the proliferation and promoted the differentiation of cortical neurons *in vivo*.

Results

AZT inhibited the proliferation of hPSC-derived neural progenitors

To determine whether AZT affected the proliferation of hPSCs, we differentiated hPSCs to dorsal telencephalic neurons spontaneously (Fig. 1*a*). The hPSC-derived neural progenitors were examined for neural stem cell markers and a newborn neuron marker, including SOX2, NESTIN, and DCX (Fig. S1). Most hPSC-derived neural progenitors were positive for these markers. Next, the hPSC-derived neural progenitors were treated with 20 or 100 μM AZT, respectively, from day 22 to day 25. At day 26, the neural progenitors were dissociated and plated for proliferation assays (Fig. 1*a*). Intriguingly, 100 μM AZT reduced the size of neurospheres significantly (Fig. 1*b*). Cell proliferation was also measured by EdU and KI67 labeling. We found that 100 μM AZT treatment reduced the EdU-labeled cells from 16.6 (control) to 9.7% (Fig. 1, *c* and *d*) and the KI67$^+$ cells from 16.8 (control) to 7.3% (Fig. 1, *e* and *f*). Furthermore, the neural progenitor markers SOX2 (control, 42.4%; 20 μM AZT, 17.3%; 100 μM AZT,7.7%) and PAX6 (control, 90.3%; 20 μM AZT, 80.3%; 100 μM AZT, 71.6%) were dramatically decreased by AZT treatment at day 28 (Fig. 1, *g–j*). Our results indicated that hPSCs pretreated with AZT for 3–6 days effectively suppressed hPSC-derived neural precursor proliferation. In addition, we tested the effect of AZT on hiPSC-derived neural progenitors (iPS cell line name, DS2U) and obtained similar results showing that AZT inhibited the proliferation of neural progenitors derived from hiPSCs (Fig. S2, *a–c*).

We also compared the effect of AZT with current known tool compounds for enhancing the differentiation of neurons. The effects of AZT and the GSI *N*-[*N*-(3,5-difluorophenacetyl)-L-alanyl]-*S*-phenylglycine *t*-butyl ester (DAPT) were tested in our system. Consistent with a previous report (16), DAPT inhibited the proliferation of neural progenitors. AZT showed a similar effect of inhibition as DAPT (Fig. S2*d*).

AZT inhibited the proliferation of hPSC-derived neural progenitors through the decrease of telomerase activity

To understand the potential mechanism of AZT-suppressed hPSC-derived neural precursor proliferation, we first tested whether AZT-suppressed hPSC-derived neural precursor proliferation was due to AZT-induced cell death. We measured cell death by TUNEL and Cell Counting Kit-8 (CCK-8) assays and showed that AZT treatment did not induce cell death *in vitro* (Fig. 1, *k* and *l*), which suggested that the AZT-suppressed cell growth was not through killing hPSC-derived cells.

To explore whether AZT inhibited the activity of telomerase in hPSCs, we tested the telomerase activity in AZT-treated hPSC-derived neural progenitors. AZT-treated cells showed a significant decrease in telomerase activity (Fig. S3*a*). Furthermore, we found that AZT inhibited the expression of telomerase-associated genes *hTEP1*, *hTER*, *TERF1*, and *TERF2IP* as well as DNA-binding and mitotic cell cycle–associated genes *DDIT3*, *CCNA1*, and *CDKN1A* compared with the controls (Fig. S3*b*).

Taken together, our results showed that AZT significantly inhibited hPSCs-derived cell proliferation through inhibiting telomerase activity, but not inducing cell death.

AZT promoted the differentiation and maturation of hPSC-derived cortical neurons

Cell differentiation and maturation are critical aspects for disease modeling and cell therapy of hPSC-derived cortical neurons. We investigated whether AZT affected the differentiation of hPSC-derived cortical neurons. The dorsal telencephalic progenitors were treated with 100 μM AZT for 6 days and plated for differentiation analysis. The TBR2$^+$ cortical progenitors were dramatically increased from 25.4 to 56.75% at day 28 (Fig. 2, *a* and *b*). In addition, markers of cortical layers, TBR1 (control, 50.1%; AZT, 74.2%), CTIP2 (control, 38.5%; AZT, 66.2%), and SATB2 (control, 13.9%; AZT, 39.2%), were also significantly increased by AZT treatment (Fig. 2, *c–h*). Our results suggested that AZT significantly enhanced the differentiation of cortical neurons. We also examined whether AZT promoted the generation of astrocytes. However, we only found a small population of hESC-derived glial fibrillary acidic protein (GFAP)–positive cells (less than 1%) at day 80 using methods described previously (5) (Fig. S4), consistent with previously reported work showing that human glial cells require a long time to differentiate. Thus, the effect of AZT on the differentiation of astrocytes was still unclear.

Next, we asked whether AZT promoted the maturation of hPSC-derived neurons. After 6 days of AZT treatment (3 days before and after cell plating on day 26), the percentages of TUJ-1$^+$ (a marker for neurons) and MAP2$^+$ (a marker for mature neurons) cells were increased by AZT treatment at day 35 (Fig. 3, *a–c*). The length of neurites (control, 88.22 μm; 20 μM AZT, 107.40 μm; 100 μM AZT, 118.80 μm), number of primary branches (control, 2.94; 20 μM AZT, 4.25; 100 μM AZT, 4.47), and average length of primary neurites (control, 67.33 μm; 20 μM AZT, 67.83 μm; 100 μM AZT, 96.57 μm) were significantly increased (Fig. 3, *d–f*), which indicated increased maturation in neural morphology in the AZT-treated group.

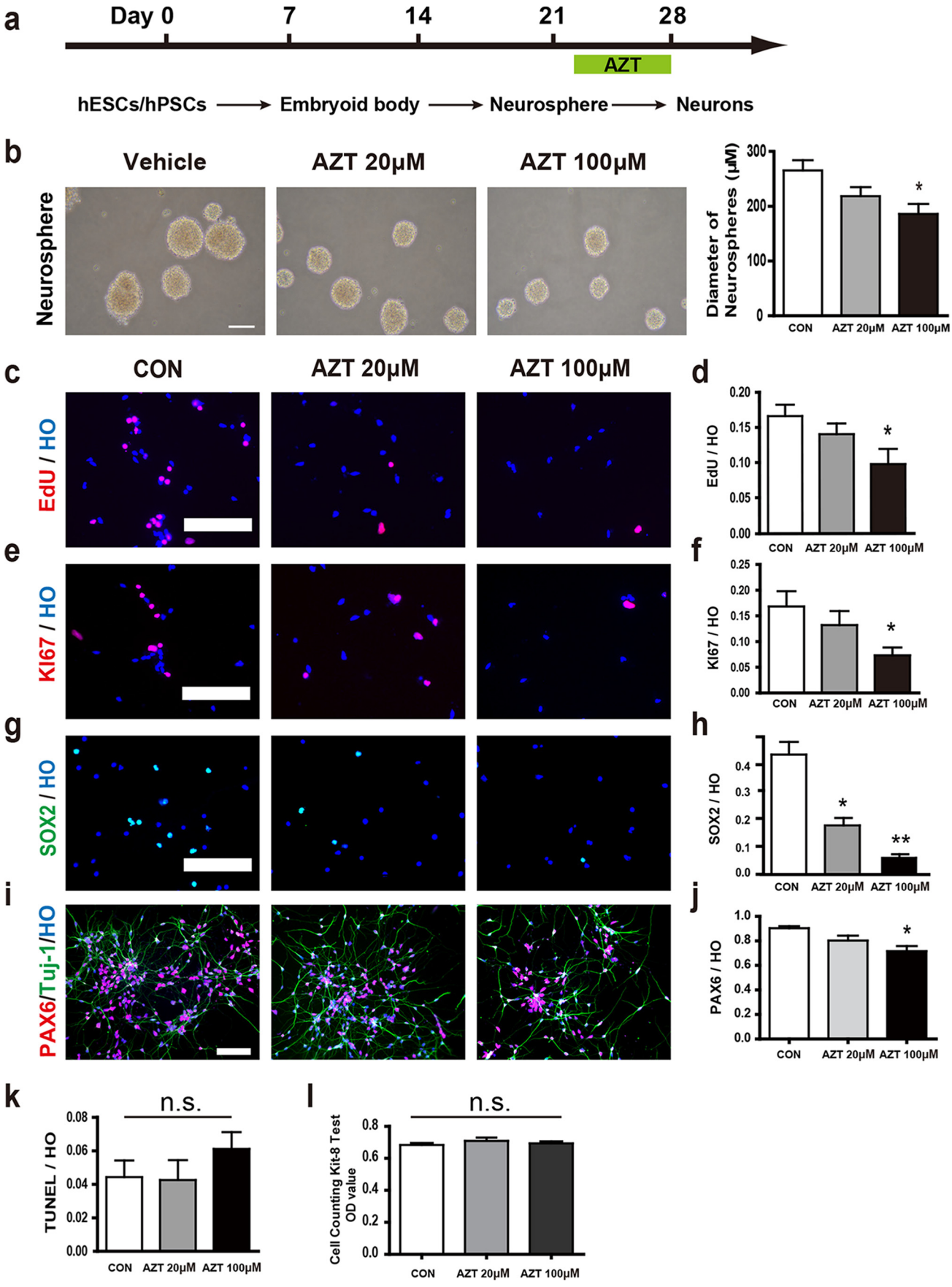
a
Day 0
7
14
21
28
AZT
hESCs/hPSCs
Embryoid body
Neurosphere
Neurons
b
Vehicle
AZT 20μM
AZT 100μM
Neurosphere
Diameter of Neurospheres (μM)
CON
AZT 20μM
AZT 100μM
c
CON
AZT 20μM
AZT 100μM
EdU / HO
d
EdU / HO
e
KI67 / HO
f
KI67 / HO
g
SOX2 / HO
h
SOX2 / HO
i
PAX6/Tuj-1/HO
j
PAX6 / HO
k
TUNEL / HO
n.s.
l
Cell Counting Kit-8 Test OD value
n.s.

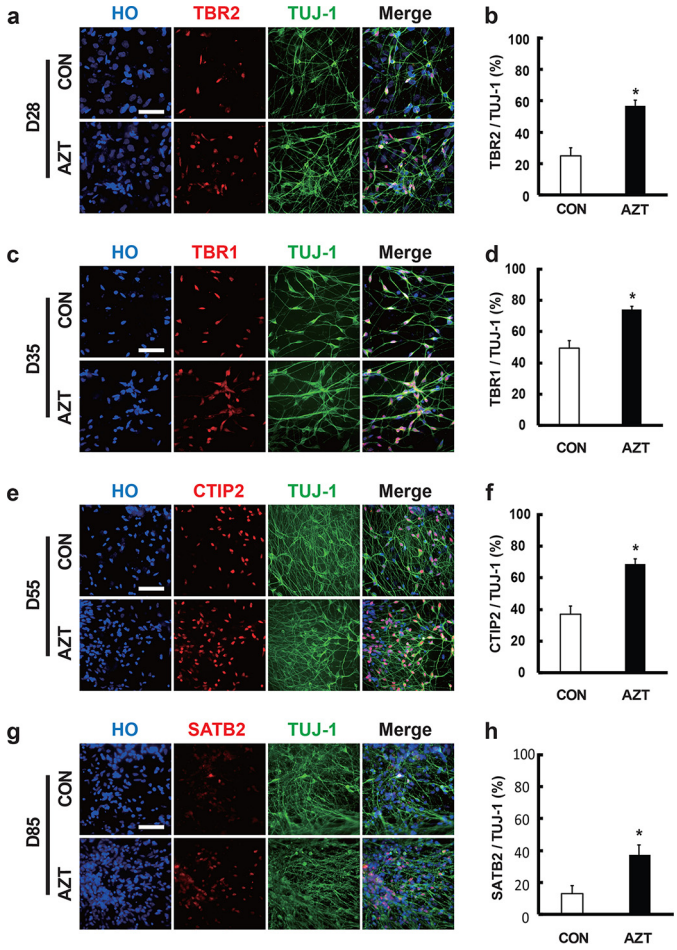

Figure 2. AZT promoted the differentiation of hPSC-derived cortical neurons. *a* and *b*, immunostaining of adherent cells at day 28 (*D28*) for TBR2 and TUJ-1. 100 μM AZT treatment significantly enhanced the percentage of TBR2-positive neurons. *c* and *d*, immunostaining of adherent cells at day 35 (*D35*) for TBR1 and TUJ-1. 100 μM AZT treatment significantly enhanced the percentage of TBR1-positive neurons. *e* and *f*, immunostaining of adherent cells at day 55 (*D55*) for CTIP2 and TUJ-1. 100 μM AZT treatment significantly enhanced the percentage of CTIP2-positive neurons. *g* and *h*, immunostaining of adherent cells at day 85 (*D85*) for SATB2 and TUJ-1. 100 μM AZT treatment significantly enhanced the percentage of SATB2-positive neurons. Control, $n = 4$; 100 μM AZT, $n = 6$. *, $p < 0.05$. *Scale bars*, 100 μm. *CON* represents control. *Error bars* represent S.E.

To further test maturation of the neurons, we measured vGLUT1 (a marker for glutamatergic transporter) and synaptophysin (a presynaptic marker) at day 95. The vGLUT1$^+$ puncta and vGLUT1$^+$ puncta among synaptophysin$^+$ puncta were significantly increased by AZT treatment (Fig. 3, *g–j*). The density of synaptophysin$^+$ puncta was also significantly enhanced by AZT treatment (Fig. 3*k*). In addition, we tested whether AZT affected the generation and maturation of ventral GABAergic neurons. The iPSC-derived ventral progenitors were treated with AZT (our established protocol (21); iPS cell line name, ihtc). Similar to cortical progenitors, the percentage of KI67$^+$ cells significantly decreased, and that of MAP2-positive neurons significantly increased (Fig. S5). Thus, AZT also promoted the maturation of GABAergic neurons significantly.

Electrophysiological characteristics correlated well with the maturation status of neurons. Thus, we examined the electrophysiological activities of AZT-treated neurons. The whole-cell clamp was performed on 7–10-day plated neurons. The inward and outward currents were recorded by using voltage-clamp steps from −80 to 60 mV (Fig. 3*m*). The membrane input conductance (control, 6.94 nanosiemens; AZT, 10.82 nanosiemens) and amplitude of Na^+ currents (control, 470.6 pA; AZT, 823.2 pA) and K^+ currents (control, 18.49 pA; AZT, 55.96 pA) were enhanced by AZT treatment (Fig. 3, *n–p*). Current-clamp recordings show that current injection (10 pA) elicited significantly more and larger action potentials in AZT-treated neurons (control, 13.1 mV; AZT, 31.7 mV), suggesting that these neurons are functionally more mature than the neurons from the control group (Fig. 3, *q–s*). Taken together, AZT promoted the maturation of hPSC-derived neurons *in vitro*.

AZT-pretreated hPSCs did not show cell overgrowth after transplantation in vivo

Cell overgrowth post-transplantation causes a high risk for tumor formation in humans and is a major concern for hPSC-based cell therapy. The effective inhibition of cell overgrowth post-transplantation is essential for translating cell therapy to the clinic. Therefore, we tested whether AZT inhibited cell overgrowth *in vivo*. We pretreated hPSC-derived neural progenitors with AZT prior to transplantation and measured cell proliferation and differentiated progeny 4 weeks postinjection (Fig. 4*a*) (four mice in each group). The brain weight among each group did not show significant differences, and no tumor formation was observed for all hPSC-transplanted mouse brains (Fig. S6*a*). The transplanted hPSC-derived neurons survived in mouse brains, and most cells showed a dispersed distribution (Fig. 4*b*). Among dispersed cells, KI67 was rarely detected in HN$^+$ (human nuclei; a marker for human nuclei) cells (less than 1%) (Fig. 4*b*), and no significant difference was found between the two groups. However, 5% of the graft area showed a rosette structure, indicating immature neural progenitors (Fig. 4*c*). Thus, we analyzed cell proliferation among the rosette structures. The percentage of PH3 (a marker expressed at late G_2 phase and throughout M phase during cell division) in HN$^+$ cells was reduced to 62.3% with AZT treatment compared with 80.8% in the control group (Fig. 4, *c* and *d*). In addition, the KI67$^+$ cells dramatically decreased upon AZT treatment (Fig. 4, *e* and *f*). The proportion of PROX1$^+$ (a

Figure 1. AZT inhibited the proliferation of hPSC-derived neural progenitors. *a*, brief time line of human stem cell differentiation for generating cortical neurons. *b*, brightfield images of neurospheres. 100 μM AZT treatment significantly reduced the diameter of neurospheres. *Scale bar*, 250 μm. *c* and *d*, EdU incorporation in adherent cells at day 28. 100 μM AZT treatment significantly reduced the percentage of EdU-incorporated cells (EdU/Hoechst). *e* and *f*, immunostaining of adherent cells at day 28 for KI67. 100 μM AZT treatment significantly reduced the percentage of KI67-positive cells (KI67/Hoechst). *g* and *h*, immunostaining of adherent cells at days 28 and 35 for SOX2. 20 and 100 μM AZT treatments significantly reduced the percentage of SOX2-positive cells (SOX2/Hoechst) at day 28. AZT treatment abolished SOX2 expression in cells at day 35. *i* and *j*, immunostaining of adherent cells at day 28 for PAX6. 100 μM AZT treatment significantly reduced the percentage of PAX6-positive cells (PAX6/Hoechst). *k*, labeling of adherent cells at day 28 for TUNEL. Neither 20 nor 100 μM AZT treatment increased the percentage of TUNEL-positive cells (TUNEL/Hoechst). *l*, CCK-8 assay of adherent cells at day 28. Neither 20 nor 100 μM AZT treatment increased the OD value of CCK-8 test. Control, $n = 5$; 20 μM AZT, $n = 5$; 100 μM AZT, $n = 6$. *, $p < 0.05$; **, $p < 0.01$; *n.s.*, not significant. *Scale bars*, 100 μm. *CON* represents control. *HO* represents Hoechst. *Error bars* represent S.E.

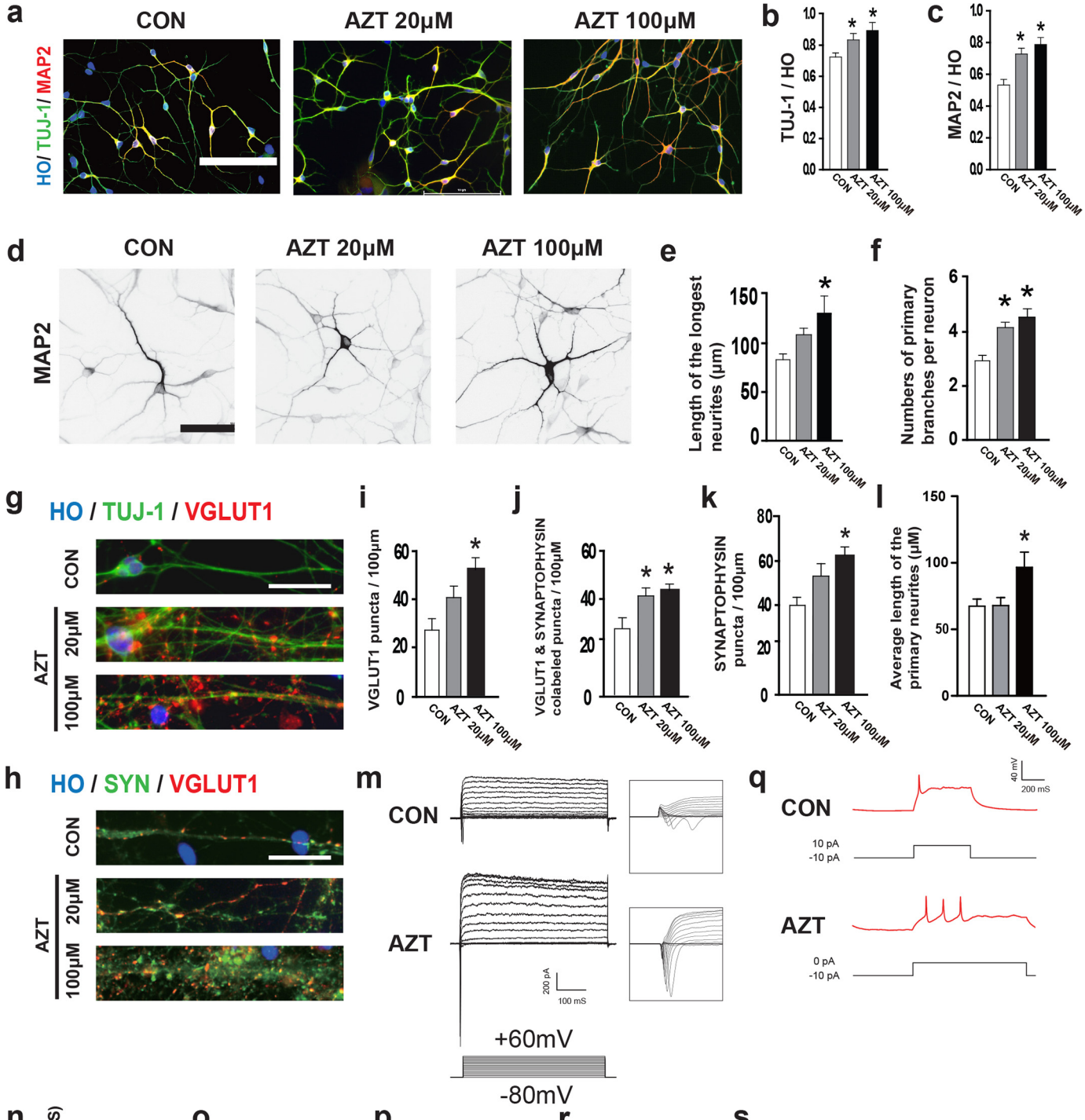
a
CON
AZT 20μM
AZT 100μM
HO/ TUJ-1/ MAP2
b
TUJ-1 / HO
c
MAP2 / HO
d
CON
AZT 20μM
AZT 100μM
MAP2
e
Length of the longest neurites (μm)
f
Numbers of primary branches per neuron
g
HO / TUJ-1 / VGLUT1
CON
AZT 20μM
AZT 100μM
i
VGLUT1 puncta / 100μm
j
VGLUT1 & SYNAPTOPHYSIN colabeled puncta / 100μM
k
SYNAPTOPHYSIN puncta / 100μm
l
Average length of the primary neurites (μM)
h
HO / SYN / VGLUT1
m
CON
AZT
200 pA
100 mS
+60mV
-80mV
q
CON
AZT
40 mV
200 mS
10 pA
-10 pA
0 pA
-10 pA
n
membrane input conductance (nS)
o
INa (pA)
p
IK (pA)
r
Numbers of AP's Fired
s
Action potential Amplitude(mV)

marker for hippocampal granule cells) cells was increased from 22.03 to 45.11% (Fig. 4, *g* and *h*), which indicated that more grafted cells became postmitotic upon AZT treatment. At 10 weeks post-transplantation (four mice in each group), most rosette structures were barely observed, and the percentage of $KI67^+$ cells among HN^+ cells in the AZT-pretreated group was dramatically decreased to less than 1% (Fig. 4*i*), whereas there were still 2.9% KI67-positive cells in the control group. Altogether, the AZT-pretreated, hPSC-derived neurons showed decreased proliferation in mouse brain post-transplantation, which suggested that AZT may effectively improve the safety of hPSC-based cell therapy.

AZT pretreatment enhanced the differentiation of cortical neurons from hPSC-derived cortical progenitors in vivo

The hPSC-based cell treatment also requires that hPSCs can differentiate into certain types of neurons, such as cortical neurons. Therefore, we evaluated the differentiation of grafted cortical neurons *in vivo* 4 weeks post-transplantation. Most transplanted human cells coexpressed HN and TUJ1 (Fig. 5*a*). AZT pretreatment significantly reduced the percentage of PAX6 (control, 48.4%; AZT, 9.45%) and FOXG1 (control, 50.1%; AZT, 29.0%) in the graft area (Fig. 5, *b–e*), which indicated a decrease of neural precursor cells. In contrast, the cortical layer markers, TBR1 (control, 49.2%; AZT, 66.3%) and CTIP2 (control, 52.9%; AZT, 73.1%), were significantly increased in the AZT-pretreated group, which suggested that AZT promoted the differentiation of cortical neurons post-transplantation (Fig. 5, *f–i*). Taken together, AZT pretreatment significantly suppressed hPSC-derived neural precursor proliferation and promoted neural differentiation *in vivo*.

Discussion

In this study, we discovered the effects of a small molecule, AZT, a telomerase inhibitor, on cell proliferation and neural differentiation of hPSC-derived neurons. AZT inhibited the proliferation of hPSC-derived neural progenitors, promoted the differentiation of hPSC-derived cortical neurons, and enhanced the maturation of hPSC-derived neurons (Fig. 6). AZT pretreatment also significantly reduced cell proliferation post-transplantation but increased mature neurons *in vivo* (Fig. 6).

Few studies of the function of telomerase in regulating the proliferation and neural differentiation of hPSC-derived neural cells have been reported. AZT interrupted cell proliferation by inhibiting TERT. Previous work showed that AZT disrupted the proliferation of adult neural stem cells in the subventricular zone and hippocampus in mice without causing cell damage or apoptosis (19, 20). Our study showed that AZT reduced the undifferentiated cells from hPSC-derived neural progenitors and promoted neural differentiation and maturation effectively both *in vitro* and *in vivo*. However, the mechanism of AZT promoting neural differentiation is still not clear. AZT is incorporated into DNA in place of thymidine, terminates early DNA synthesis, and inhibits reverse transcriptase activity during viral DNA synthesis. AZT is also an effective telomerase inhibitor. These effects may be due to AZT inhibiting cell proliferation or the important role of telomerase in neural differentiation. More efforts are needed to understand how AZT regulates neural differentiation and the function of telomerase in hPSC-derived neuron differentiation.

Previous studies have shown that inhibiting Notch signaling promoted differentiation of neural progenitor cells derived from human iPSCs (14, 16). GSIs inhibited Notch signaling in human-induced pluripotent stem cell–derived neural progenitors. A marked reduction in the percentage of dividing cells and increased neural maturation were detected in GSI-treated samples *in vitro*. Grafts from hPSCs pretreated with GSIs were significantly smaller. GSIs not only reduced the graft volume but also altered the composition of the graft. GSI-treated samples developed into mature neural grafts. Improved cell quality and safety, particularly with respect to the risk of tumor-like overgrowth, are crucial for any clinical application of hiPSC-NS/PCs. However, application of GSI caused detrimental effects in Alzheimer's disease patients (22). The toxic side effects of GSI were mainly ascribed to the inhibition of the physical functions of γ-secretase, such as the Notch signaling pathway. In clinical trials, a severe side effect of GSI treatment was worsening memory in patients (22). It also increased the risk of skin cancer, which also likely resulted from Notch signal inhibition (23). Compared with GSI, AZT is a safe and efficacious antiretroviral drug that is recommended to reduce the risk of HIV vertical transmission in pregnant women according to medical guidelines (24, 25). AZT is a widely used drug to prevent or treat HIV/AIDS, is commonly used in pregnancy clinically, and appears to be safe for the infant, suggesting it could be safe for developing organs. Moreover, we applied AZT treatment to the cell culture system before transplantation, and this *in vitro* application was not harmful. However, with AZT treatment, telomerase may potentially be translocated from the nucleus to mitochondria after induction by high-dosage AZT

Figure 3. AZT promoted dendritic and synaptic maturation of neurons. *a*, immunostaining of adherent cells at day 35 for MAP2 and TUJ-1. *b* and *c*, 20 and 100 μM AZT treatments significantly enhanced the percentage of TUJ-1–positive cells and MAP2-positive neurons (MAP2/Hoechst and MAP2/TUJ-1) at day 35. *d*, representative image for MAP2 immunostaining in adherent cells at day 35. Cells equally expressing MAP2 were subjected to morphological analysis. *e*, 100 μM AZT treatment of cells significantly increased the length of the longest neurites in D95 neurons. *f*, 20 and 100 μM AZT–treated neurons showed more primary branches at day 95 compared with control group neurons. *g* and *h*, immunostaining of adherent cells at day 95 for vGLUT1, TUJ-1, and synaptophysin. *e–g* and *i*, 100 μM AZT–treated neurons showed significantly increased vGLUT1 puncta. *j*, 20 and 100 μM AZT treatments of neurons enhanced vGLUT1- and synaptophysin-colabeled puncta significantly. *k*, 100 μM AZT–treated neurons showed significantly increased synaptophysin puncta. *l*, 100 μM AZT–treated neurons showed significantly enhanced average length of the primary neurites. *m*, Na^+/K^+ currents were recorded in voltage-clamp mode by step depolarizations from −80 to 60 mV from a holding potential of −80 mV. *n*, membrane input conductance by calculating the linear function of injected current response against membrane potential. *o*, peak Na^+ current (*INa*) showed slight enhancement in the AZT-pretreated group compared with the control group. *p*, peak K^+ current (*IK*) showed a significant increase in the AZT-pretreated group compared with the control group. *q*, representative current-clamp recordings in the control group and AZT-pretreated neurons. *r*, the numbers of action potentials (*APs*) in response to current injection. *s*, the mean action potential amplitude in response to current injection. Control, $n = 4$; 20 μM AZT, $n = 4$; 100 μM AZT, $n = 5$. *, $p < 0.05$. *Scale bars*, 100 (*a*), 50 (*d*), and 25 (*g* and *h*) μm. *SYN*, synaptophysin; *nS*, nanosiemens. *CON* represents control. *HO* represents Hoechst. *Error bars* represent S.E.

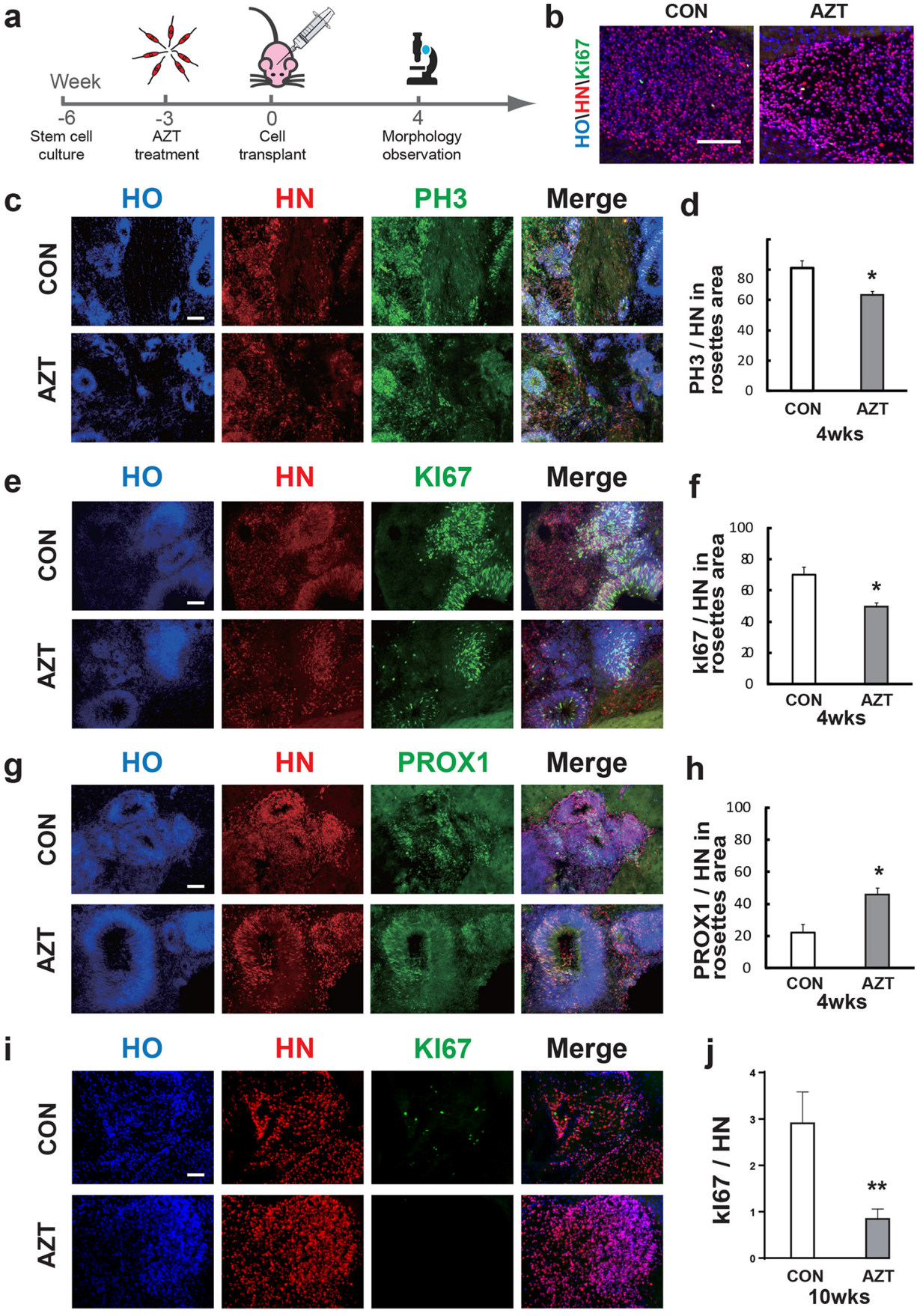
a
Week
-6
Stem cell culture
-3
AZT treatment
0
Cell transplant
4
Morphology observation
b
CON
AZT
HO\HN\Ki67
c
HO
HN
PH3
Merge
CON
AZT
d
PH3 / HN in rosettes area
80
60
40
20
0
*
CON
AZT
4wks
e
HO
HN
KI67
Merge
CON
AZT
f
KI67 / HN in rosettes area
100
80
60
40
20
0
*
CON
AZT
4wks
g
HO
HN
PROX1
Merge
CON
AZT
h
PROX1 / HN in rosettes area
100
80
60
40
20
0
*
CON
AZT
4wks
i
HO
HN
KI67
Merge
CON
AZT
j
KI67 / HN
4
3
2
1
0
**
CON
AZT
10wks

and cause mitochondrial damage (26). This effect might be a concern for using AZT as an antiproliferative tool for regenerative medicine in the clinic. Besides cell transplantation therapy, dedifferentiation in the central nervous system for neural regeneration may also cause cell overgrowth, and treatment of redifferentiating cells with AZT may reduce the risk for tumor generation.

In conclusion, we identified that the small molecule AZT plays an important role in reducing the proportion of dividing cells and increasing neural maturation (Fig. 6). AZT also prevented the tumor-like overgrowth of transplanted cells by inhibiting cell proliferation and promoting neural differentiation, which may lead to safe and long-lasting functional recovery *in vivo*. AZT would be a powerful tool to promote the hPSC-derived neural differentiation process and improve the safety of hPSC transplantation therapy.

Experimental procedures

Cell culture

hPSCs (H9, passages 35–67, WiCell Agreement 16-W0060; DS2U, passages 56–62, a kind gift from Dr. Anita Bhattacharyya (27), Waisman Center and WiCell Research Institute) were used for *in vivo* and *in vitro* studies. hPSCs were cultured under feeder-free conditions on plates coated with vitronectin (Thermo Fisher Scientific) and maintained in Essential 8 medium (Thermo Fisher Scientific) as described previously (28). Cells were passaged every 4–5 days at 80% density using EDTA (Lonza) for 1 min.

Derivation of cortical neurons from hPSCs

To induce cortical neurons, we used a procedure described previously (21, 29). Briefly, hESC clones were detached by Dispase (Thermo Fisher Scientific) to form embryoid bodies and cultured in a flask with neural induction medium (NIM) (day 0). At day 7, embryoid bodies were attached on 6-well plates. Rosette structures were observed at days 10–16. At day 16, rosettes were detached manually using a 1-ml pipette. Neuroepithelial cells were transferred into a new flask and floating cultured with NIM. At day 28, neurospheres were dissociated into single cells using TripLE (Thermo Fisher Scientific) and plated on Matrigel (BE Biosciences)- and poly-L-ornithine (Sigma)–precoated coverslips at a density of 50,000 cells/coverslip. Neurons were treated with AZT on days 22–25. After plating, AZT remained in the differentiated medium until day 28.

Transplantation

SCID (severe combined immunodeficient) mice were purchased from the Model Animal Research Center of Nanjing University. Mice were cared for following local ethics legislation for animal experimentation. Animal welfare and experimental procedures were conducted with the approval of the Institutional Animal Care and Use Committee of the Model Animal Research Center in Nanjing Medical University. For cell transplantation, day 42 neurospheres were broken into small clusters and suspended in 10–20 μl of NIM with B27 (1:50; Thermo Fisher Scientific) and penicillin (1:100; Thermo Fisher Scientific) as described previously (4, 8). The P0 SCID mice were randomly divided into two groups and anesthetized on ice for 5 s. The mice were injected with ~10,000 AZT-treated cells (neurospheres were treated with AZT on days 22–29) or nontreated cells separately in basal forebrain using a pulled glass micropipette. After injection, mice were put on a prewarmed cushion for 15 min and then put back into cages. Four or 10 weeks after transplantation, animals were perfused with 4% paraformaldehyde.

TUNEL assay and EdU cell proliferation assay

For the TUNEL assay, cortical neurons on coverslips were fixed in 4% paraformaldehyde. Apoptotic cells were detected using a Roche In Situ Cell Death Detection kit (Roche Applied Science). The EdU assay was performed using a Click-iT® EdU Alexa Fluor® Imaging kit (Thermo Fisher Scientific). At day 28, cells were treated with EdU solution and incubated for 4 h, and then cells were fixed for EdU detection. DNA was stained with Hoechst.

Cell Counting Kit-8 assay

Cell suspensions (100 μl/well; about 2000 cells) were transferred to a 96-well plate, and 10 μl of the CCK-8 (Beyotime C0037) solution was added to each well of the plate. Cells were incubated in an incubator for 0.5–4 h. Absorbance at 450 μm was measured using a microplate reader.

Immunocytochemistry

Cortical neurons on coverslips were fixed in 4% paraformaldehyde for 30 min and washed with PBS three times. Brain tissues were fixed in 4% paraformaldehyde, frozen, and sliced into 35-μm-thick slices with a Leica CM1900 rapid sectioning cryostat. Immunostaining was performed as described previously (4). Nuclei were stained with Hoechst. The primary antibodies used in this study included KI67(1:500; rabbit IgG; Zymed Laboratories Inc.), SOX2 (1:1000; rabbit IgG; Abcam), PAX6 (1:1000; rabbit IgG; Developmental Studies Hybridoma Bank), TUJ-1 (1:1000; mouse IgG; Sigma-Aldrich), TBR2 (1:500; rabbit IgG; Abcam), TBR1 (1:500; rabbit IgG; Abcam), CTIP2 (1:500; rat IgG; Abcam), SATB2 (1:500; mouse IgG; Abcam), vGLUT1 (1:500; mouse IgG; Synaptic Systems), synaptophysin (1:500; rabbit IgG; Abcam), PH3 (1:1000; rabbit IgG; Millipore), PROX1 (1:2000; rabbit IgG; Abcam), HN

Figure 4. Characterization of human iPSC–derived grafts in mouse brain under AZT pretreatment. *a*, schematic diagram of iPSC-derived neural progenitor transplantation to mouse brain. *b*, immunostaining of nonrosette grafted area. *c* and *d*, immunostaining of grafted cells for the proliferative marker PH3 4 weeks (*wks*) post-transplantation. Compared with the control group, the percentage of PH3-positive cells in grafts from 100 μM AZT–pretreated cells significantly decreased. *e* and *f*, immunostaining of grafted cells for the proliferative marker KI67 4 weeks post-transplantation. Compared with the control group, the percentage of KI67-positive cells in grafts from 100 μM AZT–pretreated cells significantly decreased. *g* and *h*, immunostaining of grafted cells for PROX1 (a hippocampal granule cell marker) 4 weeks post-transplantation. Compared with the control group, the percentage of PROX1-positive cells in grafts from 100 μM AZT–pretreated cells significantly increased. *i* and *j*, immunostaining of grafted cells for the proliferative marker KI67 at 10 weeks post-transplantation. Control, $n = 3$; AZT, $n = 4$. *, $p < 0.05$. *Scale bars*, 100 μm. *CON* represents control. *Error bars* represent S.E.

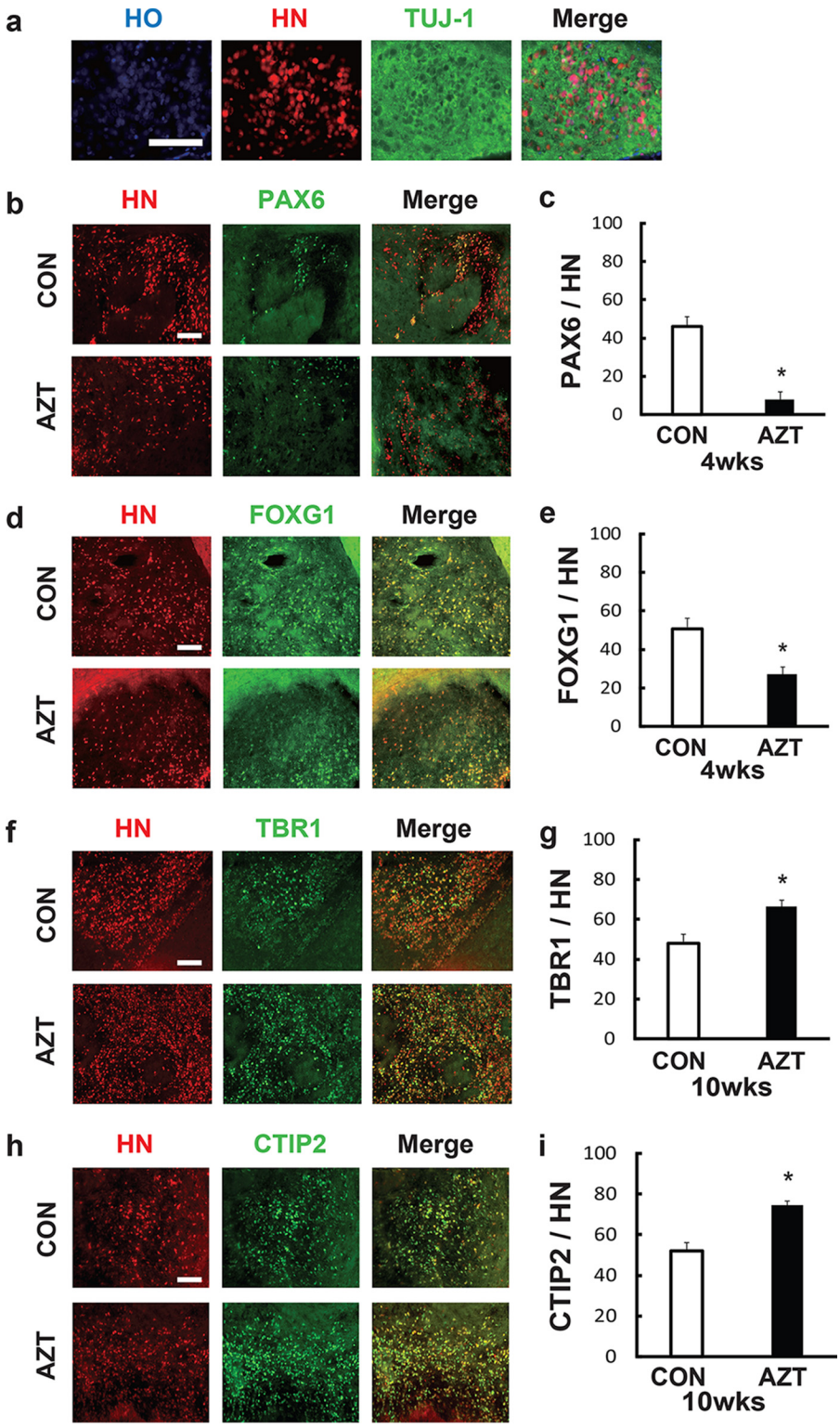

Figure 5. AZT pretreatment promoted cortical differentiation in iPSC-derived grafts. *a*, representative view of immunostaining for TUJ-1 in HN-positive grafts. The level of TUJ-1 expression was significantly higher in grafts than in the host area. *b* and *f*, immunostaining of grafted cells for PAX6, an early stage marker of neural progenitors, 4 weeks (*wks*) post-transplantation. Compared with the control group, the percentage of PAX6-positive cells in grafts from 100 μM AZT–pretreated cells significantly decreased. *c* and *g*, immunostaining of grafted cells for the early stage forebrain marker FOXG1 4 weeks post-transplantation. Compared with the control group, the percentage of FOXG1-positive cells in grafts from 100 μM AZT–pretreated cells significantly decreased. *d* and *h*, immunostaining of grafted cells for the deeper cortical layer marker TBR1 10 weeks post-transplantation. Compared with the control group, the percentage of TBR1-positive cells in grafts from 100 μM AZT–pretreated cells significantly increased. *e* and *i*, immunostaining of grafted cells for the upper cortical layer marker CTIP2 10 weeks post-transplantation. Compared with the control group, the percentage of CTIP2-positive cells in grafts from 100 μM AZT–pretreated cells significantly increased. Control, $n = 4$; AZT, $n = 4$. *, $p < 0.05$. *Scale bars*, 100 μm. *CON* represents control. *Error bars* represent S.E.

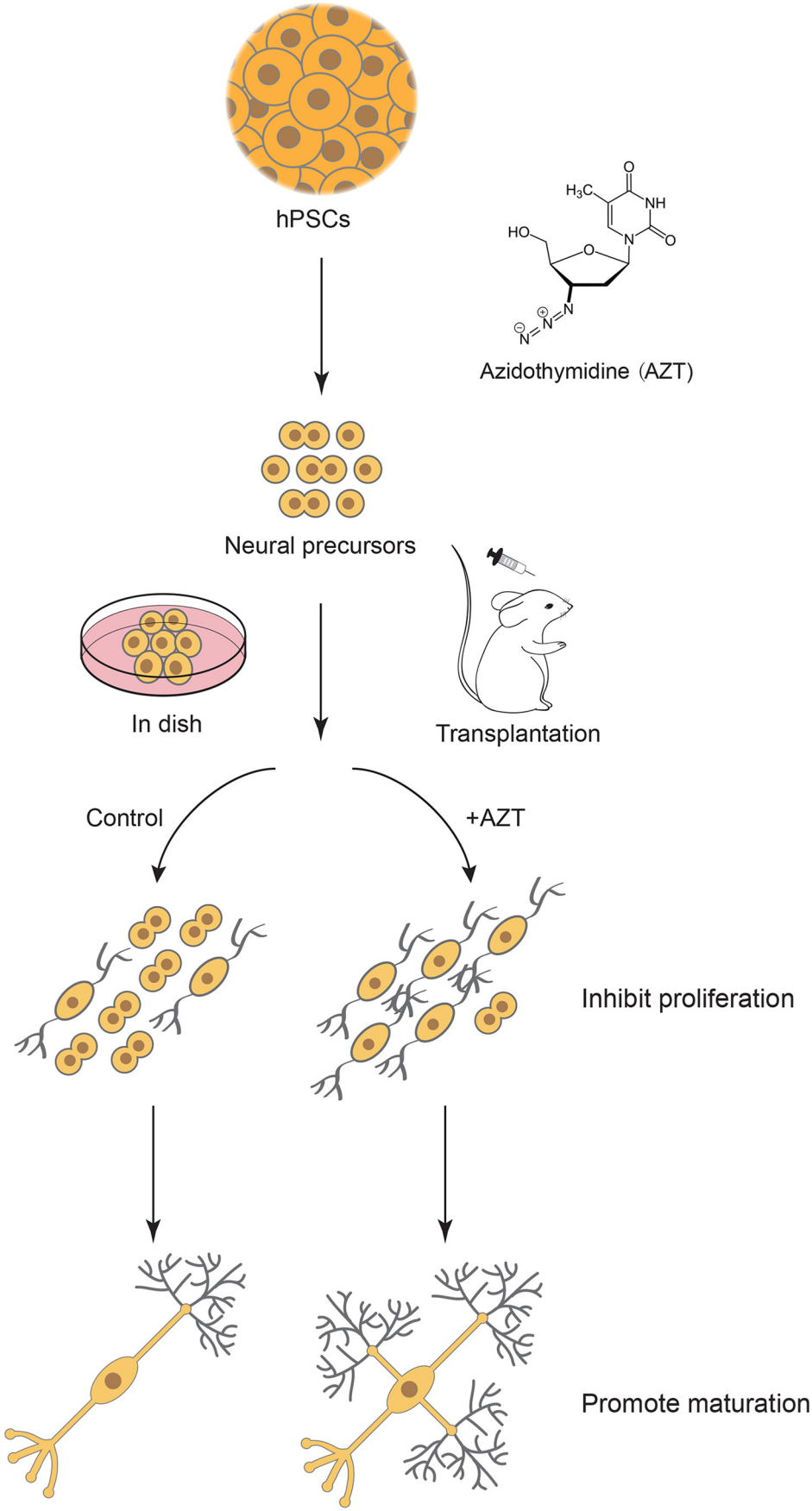

Figure 6. Schematic depicting the procedure used in this study. AZT, a telomerase inhibitor, inhibits proliferation of hPSC-derived neural progenitors, promotes differentiation of hPSC-derived cortical neurons, and induces maturation of hPSC-derived neurons both *in vitro* and *in vivo*.

(1:500; mouse IgG; Millipore), and FOXG1 (1:1000; rabbit IgG; Abcam). Coverslips were observed using a Nikon TS100 fluorescence microscope.

Neuron morphology analysis

Neurons that expressed MAP2 were randomly selected for morphology analysis. The longest neurites' pixel lengths were measured by ImageJ. Numbers of primary branches were counted manually. At least 60 neurons were analyzed randomly in every group.

Electrophysiology

Day 30 hPSC-derived neurons were cultured in a feeder-free system on Matrigel-precoated coverslips. Neurons were observed under an inverted microscope with a 60× water-immersion objective in differential interference-contrast mode. Whole-cell patch clamp recordings were made with an Olympus microscope (BX51WI), MultiClamp 700B, and Axon Digidata 1550B. Na^+/K^+ currents were recorded in voltage-clamp mode at a holding potential of −80 mV with step-voltage changes (15 steps from −80 to 60 mV). Action potentials were recorded in current-clamp mode with membrane potentials maintained around −60 mV. A series of step currents (15 steps with 10-pA increment) were injected to elicit action potentials. The pipettes were pulled by a P-1000 pipette puller (Sutter). Pipette resistance ranged from 8 to 10 megaohms. Pipettes were filled with an internal solution of 130 mM potassium gluconate, 10 mM KCl, 10 mM EGTA, 2 mM $MgCl_2$, 0.3 mM NaGTP, 2 mM Na_2ATP, and 10 mM HEPES (280 mosM, pH 7.3). The bath solution contained 145 mM NaCl, 1 mM $CaCl_2$, 5 mM KCl, 1 mM $MgCl_2$, 5 mM HEPES, and 5 mM glucose (280 mosM, pH 7.3). Data analysis was performed using Axon Clampfit software.

Quantification and statistical analysis

Quantification of fluorescence images was analyzed using ImageJ (v1.50i). At least nine fields per coverslip were chosen randomly and counted manually. Three coverslips in each group were counted. For brain slices, at least three fields were chosen. Statistical analyses were performed using GraphPad Prism (v6.01). One-way analysis of variance and Student's *t* tests were performed to statistically analyze results. $p < 0.05$ was considered to be significant. All graphical data are presented as mean ± S.E.

Author contributions—Y. H., Y. C., and Y. L. designed the experiments. K.-H. F., L.-P. S., S.-Y. C, F. Y., Y. S., M. X., and Y. H. performed the experiments. Y. H., K.-H. F., Y. P., Y. C., and Y. L. analyzed the data. Y. C. and Y. L. wrote the paper.

Acknowledgment—We thank Dr. Anita Bhattacharyya (Waisman Center and WiCell Research Institute, University of Wisconsin) for kindly gifting the DS2U iPS cell lines.

References

1. Fox, I. J., Daley, G. Q., Goldman, S. A., Huard, J., Kamp, T. J., and Trucco, M. (2014) Use of differentiated pluripotent stem cells in replacement therapy for treating disease. *Science* **345,** 1247391 CrossRef Medline
2. Nicholas, C. R., Chen, J., Tang, Y., Southwell, D. G., Chalmers, N., Vogt, D., Arnold, C. M., Chen, Y. J., Stanley, E. G., Elefanty, A. G., Sasai, Y., Alvarez-Buylla, A., Rubenstein, J. L., and Kriegstein, A. R. (2013) Functional maturation of hPSC-derived forebrain interneurons requires an extended timeline and mimics human neural development. *Cell Stem Cell* **12,** 573–586 CrossRef Medline
3. Fasano, C. A., Chambers, S. M., Lee, G., Tomishima, M. J., and Studer, L. (2010) Efficient derivation of functional floor plate tissue from human embryonic stem cells. *Cell Stem Cell* **6,** 336–347 CrossRef Medline
4. Liu, Y., Weick, J. P., Liu, H., Krencik, R., Zhang, X., Ma, L., Zhou, G. M., Ayala, M., and Zhang, S. C. (2013) Medial ganglionic eminence-like cells derived from human embryonic stem cells correct learning and memory deficits. *Nat. Biotechnol.* **31,** 440–447 CrossRef Medline
5. Krencik, R., Weick, J. P., Liu, Y., Zhang, Z. J., and Zhang, S. C. (2011) Specification of transplantable astroglial subtypes from human pluripotent stem cells. *Nat. Biotechnol.* **29,** 528–534 CrossRef Medline
6. Hu, B. Y., Du, Z. W., Li, X. J., Ayala, M., and Zhang, S. C. (2009) Human oligodendrocytes from embryonic stem cells: conserved SHH signaling networks and divergent FGF effects. *Development* **136,** 1443–1452 CrossRef Medline
7. Ma, L., Hu, B., Liu, Y., Vermilyea, S. C., Liu, H., Gao, L., Sun, Y., Zhang, X., and Zhang, S. C. (2012) Human embryonic stem cell-derived GABA neurons correct locomotion deficits in quinolinic acid-lesioned mice. *Cell Stem Cell* **10,** 455–464 CrossRef Medline
8. Weick, J. P., Liu, Y., and Zhang, S. C. (2011) Human embryonic stem cell-derived neurons adopt and regulate the activity of an established neural network. *Proc. Natl. Acad. Sci. U.S.A.* **108,** 20189–20194 CrossRef Medline
9. Kriks, S., Shim, J. W., Piao, J., Ganat, Y. M., Wakeman, D. R., Xie, Z., Carrillo-Reid, L., Auyeung, G., Antonacci, C., Buch, A., Yang, L., Beal, M. F., Surmeier, D. J., Kordower, J. H., Tabar, V., *et al.* (2011) Dopamine neurons derived from human ES cells efficiently engraft in animal models of Parkinson's disease. *Nature* **480,** 547–551 CrossRef Medline
10. Cunningham, M., Cho, J. H., Leung, A., Savvidis, G., Ahn, S., Moon, M., Lee, P. K., Han, J. J., Azimi, N., Kim, K. S., Bolshakov, V. Y., and Chung, S. (2014) hPSC-derived maturing GABAergic interneurons ameliorate seizures and abnormal behavior in epileptic mice. *Cell Stem Cell* **15,** 559–573 CrossRef Medline
11. Fattahi, F., Steinbeck, J. A., Kriks, S., Tchieu, J., Zimmer, B., Kishinevsky, S., Zeltner, N., Mica, Y., El-Nachef, W., Zhao, H., de Stanchina, E., Gershon, M. D., Grikscheit, T. C., Chen, S., and Studer, L. (2016) Deriving human ENS lineages for cell therapy and drug discovery in Hirschsprung disease. *Nature* **531,** 105–109 CrossRef Medline
12. Tao, Y., and Zhang, S. C. (2016) Neural subtype specification from human pluripotent stem cells. *Cell Stem Cell* **19,** 573–586 CrossRef Medline
13. Aubry, L., Bugi, A., Lefort, N., Rousseau, F., Peschanski, M., and Perrier, A. L. (2008) Striatal progenitors derived from human ES cells mature into DARPP32 neurons *in vitro* and in quinolinic acid-lesioned rats. *Proc. Natl. Acad. Sci. U.S.A.* **105,** 16707–16712 CrossRef Medline
14. Okubo, T., Iwanami, A., Kohyama, J., Itakura, G., Kawabata, S., Nishiyama, Y., Sugai, K., Ozaki, M., Iida, T., Matsubayashi, K., Matsumoto, M., Nakamura, M., and Okano, H. (2016) Pretreatment with a γ-secretase inhibitor prevents tumor-like overgrowth in human iPSC-derived transplants for spinal cord injury. *Stem Cell Rep.* **7,** 649–663 CrossRef Medline
15. Bardy, C., van den Hurk, M., Eames, T., Marchand, C., Hernandez, R. V., Kellogg, M., Gorris, M., Galet, B., Palomares, V., Brown, J., Bang, A. G., Mertens, J., Böhnke, L., Boyer, L., Simon, S., *et al.* (2015) Neuronal medium that supports basic synaptic functions and activity of human neurons *in vitro*. *Proc. Natl. Acad. Sci. U.S.A.* **112,** E2725–E2734 CrossRef Medline; Correction (2015) *Proc. Natl. Acad. Sci. U.S.A.* **112,** E3312 CrossRef Medline
16. Ogura, A., Morizane, A., Nakajima, Y., Miyamoto, S., and Takahashi, J. (2013) γ-Secretase inhibitors prevent overgrowth of transplanted neural progenitors derived from human-induced pluripotent stem cells. *Stem Cells Dev.* **22,** 374–382 CrossRef Medline
17. Imbimbo, B. P., and Giardina, G. A. (2011) γ-Secretase inhibitors and modulators for the treatment of Alzheimer's disease: disappointments and hopes. *Curr. Top. Med. Chem.* **11,** 1555–1570 CrossRef Medline

18. Mitsuya, H., Weinhold, K. J., Furman, P. A., St Clair, M. H., Lehrman, S. N., Gallo, R. C., Bolognesi, D., Barry, D. W., and Broder, S. (1985) 3′-Azido-3′-deoxythymidine (BW A509U): an antiviral agent that inhibits the infectivity and cytopathic effect of human T-lymphotropic virus type III/lymphadenopathy-associated virus *in vitro*. *Proc. Natl. Acad. Sci. U.S.A.* **82,** 7096–7100 CrossRef Medline
19. Zhou, Q. G., Hu, Y., Hua, Y., Hu, M., Luo, C. X., Han, X., Zhu, X. J., Wang, B., Xu, J. S., and Zhu, D. Y. (2007) Neuronal nitric oxide synthase contributes to chronic stress-induced depression by suppressing hippocampal neurogenesis. *J. Neurochem.* **103,** 1843–1854 CrossRef Medline
20. Zhou, Q. G., Hu, Y., Wu, D. L., Zhu, L. J., Chen, C., Jin, X., Luo, C. X., Wu, H. Y., Zhang, J., and Zhu, D. Y. (2011) Hippocampal telomerase is involved in the modulation of depressive behaviors. *J. Neurosci.* **31,** 12258–12269 CrossRef Medline
21. Liu, Y., Liu, H., Sauvey, C., Yao, L., Zarnowska, E. D., and Zhang, S. C. (2013) Directed differentiation of forebrain GABA interneurons from human pluripotent stem cells. *Nat. Protoc.* **8,** 1670–1679 CrossRef Medline
22. Doody, R. S., Raman, R., Farlow, M., Iwatsubo, T., Vellas, B., Joffe, S., Kieburtz, K., He, F., Sun, X., Thomas, R. G., Aisen, P. S., Alzheimer's Disease Cooperative Study Steering Committee, Siemers, E., Sethuraman, G., Mohs, R., and Semagacestat Study Group (2013) A phase 3 trial of semagacestat for treatment of Alzheimer's disease. *New Engl. J. Med.* **369,** 341–350 CrossRef Medline
23. Olsauskas-Kuprys, R., Zlobin, A., and Osipo, C. (2013) γ secretase inhibitors of Notch signaling. *Onco Targets Ther.* **6,** 943–955 CrossRef Medline
24. Lambert, J. S., Nogueira, S. A., Abreu, T., Machado, E. S., Costa, T. P., Bondarovsky, M., Andrade, M., Halpern, M., Barbosa, R., and Perez, M. (2003) A pilot study to evaluate the safety and feasibility of the administration of AZT/3TC fixed dose combination to HIV infected pregnant women and their infants in Rio de Janeiro, Brazil. *Sex. Transm. Infect.* **79,** 448–452 CrossRef Medline
25. Kesho Bora Study Group (2012) Maternal HIV-1 disease progression 18–24 months postdelivery according to antiretroviral prophylaxis regimen (triple-antiretroviral prophylaxis during pregnancy and breastfeeding vs zidovudine/single-dose nevirapine prophylaxis): the Kesho Bora randomized controlled trial. *Clin. Infect. Dis.* **55,** 449–460 CrossRef Medline
26. Babizhayev, M. A., and Yegorov, Y. E. (2015) Tissue formation and tissue engineering through host cell recruitment or a potential injectable cell-based biocomposite with replicative potential: molecular mechanisms controlling cellular senescence and the involvement of controlled transient telomerase activation therapies. *J. Biomed. Mater. Res. A* **103,** 3993–4023 CrossRef Medline
27. Weick, J. P., Held, D. L., Bonadurer, G. F., 3rd, Doers, M. E., Liu, Y., Maguire, C., Clark, A., Knackert, J. A., Molinarolo, K., Musser, M., Yao, L., Yin, Y., Lu, J., Zhang, X., Zhang, S. C., *et al.* (2013) Deficits in human trisomy 21 iPSCs and neurons. *Proc. Natl. Acad. Sci. U.S.A.* **110,** 9962–9967 CrossRef Medline
28. Yuan, F., Fang, K. H., Cao, S. Y., Qu, Z. Y., Li, Q., Krencik, R., Xu, M., Bhattacharyya, A., Su, Y. W., Zhu, D. Y., and Liu, Y. (2015) Efficient generation of region-specific forebrain neurons from human pluripotent stem cells under highly defined condition. *Sci. Rep.* **5,** 18550 CrossRef Medline
29. Pankratz, M. T., Li, X. J., Lavaute, T. M., Lyons, E. A., Chen, X., and Zhang, S. C. (2007) Directed neural differentiation of human embryonic stem cells via an obligated primitive anterior stage. *Stem Cells* **25,** 1511–1520 CrossRef Medline